La mer 41 : 94–105, 2003
Société franco-japonaise d'océanographie, Tokyo

Analysis of 3-dimensional Hydro-dynamical Model Simulation in the Gulf of Kutch, India and Its Comparison with Satellite Data

Takahiro OSAWA[1], Chaofang ZHAO[1,2], Pravin D. KUNTE[1,3], Lee Sung AE[1], Masanao HARA[4], Takashi MORIYAMA[5]

Abstract : A 3D COSMOS numerical model, initially developed by NAKATA *et al.* (1983), has been used in the Gulf of Kutch situated in the northwest of India to study tidal variation, ocean current, residual current and sea surface temperature distribution, which are very important parameters in investigating natural ecosystem and suspended matter or pollution transportation in the Gulf. Wind speed, air-sea heat flux and five main tidal components are considered in this study, and the results are compared with earlier researches (UNNIKRISHNAN *et al.*, 1999, SINHA *et al.*, 2000). The model results show that the model performs well in simulating hydro-dynamical parameters. The main features of surface current are the same as the results of SINHA *et al.* (2000) and tidal current is the main factor as compared to wind induced current due to high tidal variation. Residual current distribution owns similar features with previous studies (UNNIKRISHNAN *et al.*, 1999, SINHA *et al.*, 2000) but with a much clear eddy formation near the mouth area of the Gulf. Sea surface temperature distribution estimated from the model shows similar pattern with that measured by NOAA/AVHRR by including wind stress in the model, but salinity distribution varies little ranging from 36.09 to 36.13 PSU in our numerical model simulation.

Keywords : *3D numerical model, satellite data, dynamical parameters, residual current, sea surface temperature, Kutch, India.*

1. Introduction

Coastal area and enclosed bay are generally the most developed areas accompanied with large cities, different kinds of industries and large population activities. Domestic and industry waste discharges cause ocean pollution, heavy nourishing and then, red tide is easy to occur. Much more environmental pressures exist in these areas. The Gulf of Kutch (shown in Figure 1) , located in the northwest coast of India, is the northeastern stretch of Arabian Sea. The Gulf of Kutch has been used as the important ports from ancient India. In recent years, the Gulf of Kutch, as same with other enclosed bay in the world, faces much more marine environmental problems; especially many factories have set up around the Bay. Therefore, it is important to develop hydro-dynamical and eco-dynamical models for ocean environment management and parameter monitoring.

The Gulf of Kutch, with the area of over 7300km^2, is about 130 kilometers in east-west direction, and 30 kilometers in north-south direction at the central part of the Gulf. The mean depth of the Gulf is around 18 meters and the deepest part with depths ranging from 50–60 meters in the estuary. The main feature

1. Center for Environmental Remote Sensing, Chiba University, 33,Yayoicho, Inage, Chiba, Japan 263 8522
2. National Laboratory of Ocean Remote Sensing, Ocean University of Qingdao, 5, Yushan Road, Qingdao, P. R. China 266003
3. National Institute of Oceanography, Goa, India
4. Vision Tech Inc. 2–1–16 Umezono, Tsukuba-city, Ibaraki Japan 305–0045
5. NASDA SPPD, 2–1–1 Sengenn, Tukuba–city Ibaraki Japan 305–8505

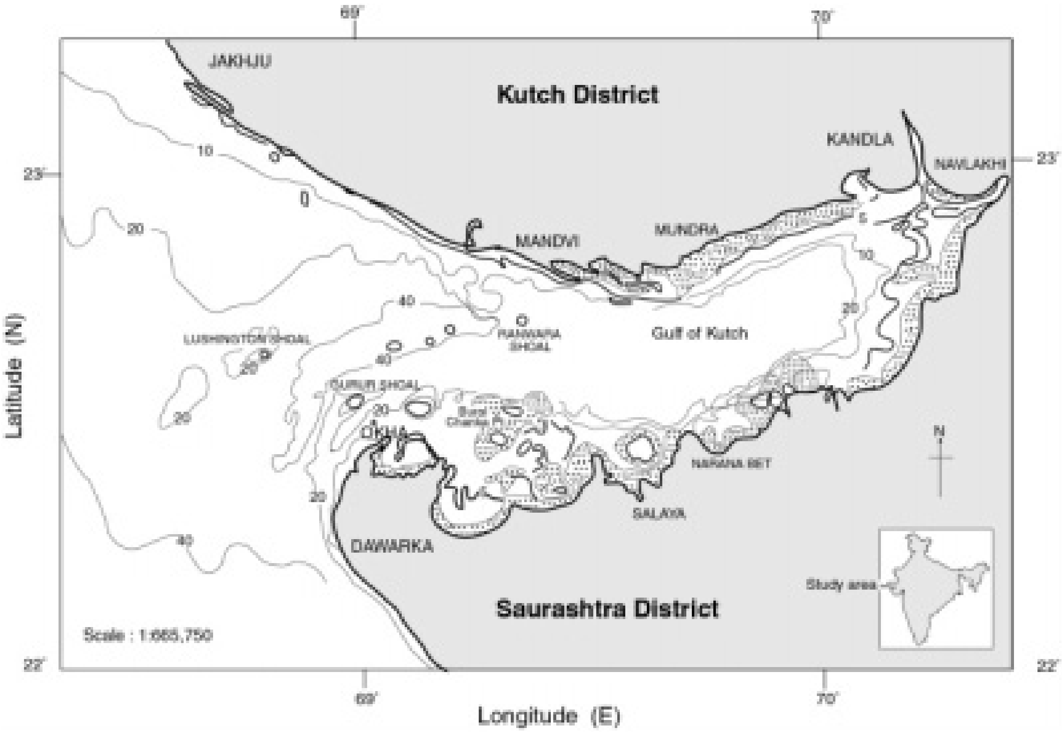

Figure 1. Location map of the Gulf of Kutch showing geomorphic features and bathymetric contours in meter.

is that the Gulf of Kutch is located in an arid zone with mean annually precipitation of about 0.4 m/year but with mean evaporation of about 1.4 m/year. Generally, salinities in the Gulf are higher than the mouth region with mean value of about 36 psu throughout the year (UNNIKSHISHMNAN *et al*, 1999). The other feature of the Gulf is with high tidal range variation. Even at Okha, located at the mouth of the Gulf, the mean spring tidal range is over 3m, and at the eastern part of the Gulf it is over 6 meters. CENTRAL ELECTRICITY AUTHORITY of India (1985) also reported that the peak surface current velocity is in the range between 0.75 to 1.25 m/s at the estuary and between 1.5 to 2.5m/s in the central part of the Gulf.

Numerical studies in the Gulf of Kutch have been carried out for many years. SALOMON (1976) and PRANDTL (1984) simulated tidal circulation using two dimensional hydrodynamic model. UNNIKRISNAN *et al.* (1999) used 2D barotropic model to study tidal regime in the Gulf of Kutch and have found that an eddy exists in M_2 residual current. They also found that a balance between the pressure gradient and the friction near the coast characterizes the dynamics of tidal propagation in the Gulf. SINHA *et al.* (2000) proposed a vertically integrated model to study tidal circulation and currents with tidal forcing along the open boundary of the model domain for the construction of the proposed tidal barrage, and pointed out the importance of the bathymetry of the Gulf simulating the current field. After considering the tidal variation in the Gulf, the CENTRAL ELECTRICITY AUTHORITY of India (1985) investigated the possibilities for tidal power development in the Gulf of Kutch. S HETYE (1999) studied the amplification of tidal amplitude in the Gulf of Kutch based on analytical and numerical model of linear, viscous, and cross-section averaged equations for tidal motion. He found that the amplification is due to a combination of quarter-wavelength resonance, geometric effect and sea bottom friction. We can see that only main tidal component and bathymetry of the Gulf were considered based on analytical or 2D numerical model in the previous studies. No any researches was reported in studying the ocean current in the subsurface layers.

In recent years, many satellites have been launched and are operating. Several environmental parameters are obtained from these satellites, such as wind velocity from European ERS and US Quickscat, sea surface temperature and cloud fraction from NOAA/AVHRR and chlorophyll concentration from SeaWiFS. These data are sometimes used to monitor the variation of environment in the enclosed Gulf. Making full use of such satellite observations and combining with numerical model simulation will give better understandings of dynamical or eco-system processes in the coastal or enclosed Gulf at the present time.

The objective of this study is to simulate dynamical parameters in the Gulf of Kutch using 3-dimensional baroclinic numerical model in order to study the impact of human activities on the eco-system environment of Gulf of Kutch. Wind speed derived from Quickscat data was used in the initial condition of the model, and NOAA/AVHRR sea surface temperature data was used for surface temperature. Compared with earlier studies, several other factors such as surface wind, air-sea heat flux and river discharge around the Gulf of Kutch are introduced in 3D numerical model (COSMOS), which was initially developed by NAKATA *et al.* (1983), in addition to 5 main tidal components are considered. Section 2 will give a brief introduction of 3-dimensional numerical model. The initial conditions used in the model will be described in Section 3. The model results and discussion will be provided in Section 4, and finally Section 5 will give the conclusions.

2. Numerical model descriptions

2.1 Fundamental equation

3-dimensional (3-D) numerical model is used in this study. This model is first developed by NAKATA *et al.* (1983) and applied in the enclosed bay such as Chinhae Bay and Tokyo Bay, etc (HORIGUCHI, *et al.*, 1998a,b). Tide, wind and river run-off are taken into account in the model. After considering Boussinesq approximation, incompressible fluid and constant Coriolis forcing, the momentum equations, equation of mass continuity, temperature and salinity conservations and state equation are summarized as follows.

$$\frac{\partial u}{\partial t} = -\frac{\partial}{\partial x}(u^2) - \frac{\partial}{\partial y}(uv) - \frac{\partial}{\partial z}(uw) + f_0 v - g\frac{\partial \zeta}{\partial x} - \frac{g}{\rho}\int_z^0 \frac{\partial \rho}{\partial x}dz' - \frac{1}{\rho}\frac{\partial P_a}{\partial x} + \frac{\partial}{\partial x}\left(N_x\frac{\partial v}{\partial x}\right) + \frac{\partial}{\partial y}\left(N_y\frac{\partial v}{\partial y}\right) + \frac{\partial}{\partial z}\left(N_z\frac{\partial v}{\partial z}\right) \quad (1)$$

$$\frac{\partial v}{\partial t} = -\frac{\partial}{\partial x}(uv) - \frac{\partial}{\partial y}(v^2) - \frac{\partial}{\partial z}(uw) - f_0 u - g\frac{\partial \zeta}{\partial y} - \frac{g}{\rho}\int_z^0 \frac{\partial \rho}{\partial y}dz' - \frac{1}{\rho}\frac{\partial P_a}{\partial y} + \frac{\partial}{\partial x}\left(N_x\frac{\partial v}{\partial y}\right) + \frac{\partial}{\partial y}\left(N_y\frac{\partial v}{\partial y}\right) + \frac{\partial}{\partial z}\left(N_z\frac{\partial v}{\partial z}\right) \quad (2)$$

$$\frac{\partial u}{\partial x} + \frac{\partial v}{\partial y} + \frac{\partial w}{\partial z} = 0, \quad (3)$$

$$\frac{\partial \zeta}{\partial t} = -\frac{\partial}{\partial x}\left(\int_{-H}^{\zeta} udz\right) - \frac{\partial}{\partial y}\left(\int_{-H}^{\zeta} vdz\right), \quad (4)$$

$$\frac{\partial T}{\partial t} = -\frac{\partial}{\partial x}(uT) - \frac{\partial}{\partial y}(vT) - \frac{\partial}{\partial z}(wT) + \frac{\partial}{\partial x}\left(k_x\frac{\partial T}{\partial x}\right) + \frac{\partial}{\partial y}\left(k_y\frac{\partial T}{\partial y}\right) + \frac{\partial}{\partial z}\left(k_z\frac{\partial T}{\partial z}\right), \quad (5)$$

and

$$\frac{\partial Cl}{\partial t} = -\frac{\partial}{\partial x}(uCl) - \frac{\partial}{\partial y}(vCl) - \frac{\partial}{\partial z}(wCl) + \frac{\partial}{\partial x}\left(k_x\frac{\partial Cl}{\partial x}\right) + \frac{\partial}{\partial y}\left(k_y\frac{\partial Cl}{\partial y}\right) + \frac{\partial}{\partial z}\left(k_z\frac{\partial Cl}{\partial z}\right), \quad (6)$$

$$\rho = \rho(Cl,\ T) \text{ and } \rho = \frac{\sigma_t}{1000} + 1 \quad (7)$$

σ_t is calculated by the following equations as,

$$\sigma_t = \sum_t + (\sigma_0 + 0.1324)\{1 - A_t + B_t(\sigma_0 + 0.1324)\}, \quad (8)$$

and

$$\sigma_0 = 0.069 + 1.4708Cl - 0.001570Cl^2 + 0.0000398Cl^3 \quad (9)$$

where,

$$\sum_t - \frac{(T - 3.98)^2}{503.570}\left[\frac{T + 283.0}{T + 67.26}\right], \quad (10)$$

$$A_t = T(4.7867-0.098185T + 0.00108437T^2)\cdot 10^{-3}, \quad (11)$$

and

$$B_t = T(18.030-0.8164T+0.01667T^2)\cdot 10^{-6}. \quad (12)$$

u and v are the horizontal current velocities in the x and y directions, respectively; w is the vertical velocity with positive upward; ζ is the surface variation; ρ is density of sea water; f_0 is the Coriolis parameter; g is the acceleration due to gravity; T and Cl are the temperature and salinity, respectively; N and k are the coefficients of eddy viscosity and diffusivity, respectively. Kundsen's state equations have been used in the model.

2.2 Boundary conditions of the model

The boundary conditions used in this model include sea surface, sea bottom friction, open boundary and the discharge from rivers along the Gulf of Kutch. At the sea surface, the average wind stress is used here.

$$\rho_0(A_z\frac{\partial U}{\partial z},\ A_z\frac{\partial V}{\partial z}) = (\tau_x,\ \tau_y) \quad (13a)$$

and

$$(\tau_x,\ \tau_y) = \rho_a C_d(UW,\ VW). \quad (13b)$$

Here ρ_0 is air density (1.2×10^{-3}g/cm^3); C_d is the drag coefficients; U, V are wind velocities in the x, y directions, respectively; W is wind speed; τ_x, τ_y are wind stress in the x, y directions, respectively.

Similarly, at the sea bottom ($z=-H$), the boundary conditions are defined as follows,

$$\rho(A_z\frac{\partial U^b}{\partial z},\ A_z\frac{\partial V^b}{\partial z}) = (\tau_x^b,\ \tau_y^b) \quad (14a)$$

and

$$(\tau_x^b,\ \tau_y^b) = \rho C_b(U^b W^b,\ V^b W^b). \quad (14b)$$

ρ is seawater density (1.024g/cm^3); (τ_x^b, τ_y^b) are frictional stresses at the sea bottom in the x, y directions, respectively; C_b is the frictional coefficient at the sea bottom. No slip condition is used at the land boundary. U^b, V^b, W^b are the current velocities in the x, y directions, and the current speed, respectively.

Heat flux between the atmosphere and ocean is estimated from two heat exchange processes. One is the heating process including short wave radiation from sun, and long wave radiation from the atmosphere, and the other is cooling process including latent heat flux by water evaporation, and sensible heat exchange. The total heat flux could be estimated from sea surface temperature, air temperature, relative humidity, cloud content, and wind speed. All these data are obtained from Da SILVA *et al.* (1994) excerpt sea surface temperature (SST) and wind speed, where SST is estimated from NOAA/AVHRR data, and wind speed is estimated from Quikscat data.

As no field observation of tides in the open boundary, a composite tide is constructed in the form as follows (UNNIKRISHNAN *et al.* ,1999, NAKANO, 1936),

$$\xi(t) = z_0 + \sum A_i f_i \cos\{\sigma_t t - g_i + (V_i + u_i)\}. \quad (15)$$

z_0 is the mean sea level; A_i and g_i are the amplitude and Greenwich phase of the constitute i, respectively; f_i is node factor; (V_i+u_i) is the astronomical arguments; σ_t is the tidal frequency. The amplitudes and Greenwich phases of various constituents at several stations around the Gulf of Kutch are documented by the International Hydrographic Bureau, Monaco (UNNIKRISHNAN *et al.*, 1999), and the astronomical arguments can be calculated theoretically and here the data are excerpted from NAKANO (1936). Table 2 lists all the five tidal components of M_2, S_2, N_2, K_1 and O_1 considered in this study.

3. Model calculation conditions

In the application of model to the Gulf of Kutch, the model domain (69.82°–70.46°E, 22.26°–23.00°N) covers the whole Gulf with 37 grids in north-south direction and 78 grids in west-east direction. The grid resolution is 2000 meters in both directions, and the time-step is 30 seconds. The Gulf is divided into 5 layers in the vertical direction with layer thicknesses being 5 meters in the first 3 layers, and 10 meters for the fourth layer. The last layer is set from 25 m to the bottom. The coefficients of eddy viscosity and diffusivity are taken to be equal to 0.85 m^2/s as used by UNNIKRISHNAN *et al.* (1999). The coefficient of the vertical eddy diffusivity is set to 1.0 cm^2/s (HORIGUCHI *et al.*, 1998a, NAKATA *et al.*, 1983).

At the open boundary, the mean sea level at the Gulf estuary is set to 0.01 m, which is used for tidal forcing. Compared with previous

Table 1. Simulation conditions used in Gulf of Kutch

Items		Contents
1. Grids		77x38 grids Grid resolution: 2 km
2. Layers		First layer 0–5 m 2nd layer 5–10 m 3rd layer 10–15 m 4th layer 15–25 m 5th layer 25–bottom
3. Open boundary	Tide conditions	M_2, S_2, N_2, K_1, O_1 components are considered, the parameters are shown in table 2.
	Temperature and salinity profile	The in situ data measured in 1997 is used shown in Fig. 2c
4. Other Parameters	Coriolis coefficient (f)	5.62E−5 s^{-1}
	Bottom friction coefficient (C_b)	0.0026
	Surface friction coefficient (C_b)	0.0013
	Coefficient of eddy viscosity (horizontal) (N)	8.5E+5 cm^2 s^{-1}
	Coefficient of eddy diffusion (vertical) (k)	1.0 cm^2 s^{-1}
5. River Discharge		Phuldi, Machhu and Demi rivers run-off were used as shown in Table 3
6. Meteorological conditions	Wind velocity	Wind velocity data retrieved from Quikscat stions ensor are used and shown in Fig. 2a and Table 4
	Solar irradiance	711 cal/cm^2
	Solar zenith	0.84
	Air temperature	26.4
	Relative humidity	68.7%
	Cloud fraction	0.11
7. Time step	30 seconds	30 days from Nov.1—30, 1999

Table 2. Tide components data used in this research

Tide components	Period (hours)	Amplitude $A_i f_i$ (cm)	Phase (degree) $-g_i+(V_i+u_i)$
M_2	12.4	116.4	−5.01
S_2	12.0	33.5	151.36
N_2	12.7	39.5	80.85
K_1	23.9	25.7	124.35
O_1	26.9	17.4	53.64

Table 3. Main river input to the Gulf of Kutch in m^3/s and the last three rivers are considered in the numerical model

Adhoi	2.1
Sakara	4.0
Jhinhjoda	1.0
Phuldi	24.0
Machhu	476.0
Demi	438.0

studies, here we considered five main tidal components in the model, and the harmonic coefficients and the phase as shown in equation (15) are summarized in Table 2. As for the main river run-offs around the Gulf of Kutch, Machhu, Demi and Phuldi rivers are considered, and their volume transports are listed in Table 3.

The other meteorological conditions are wind velocity over the Gulf, solar irradiance, day-

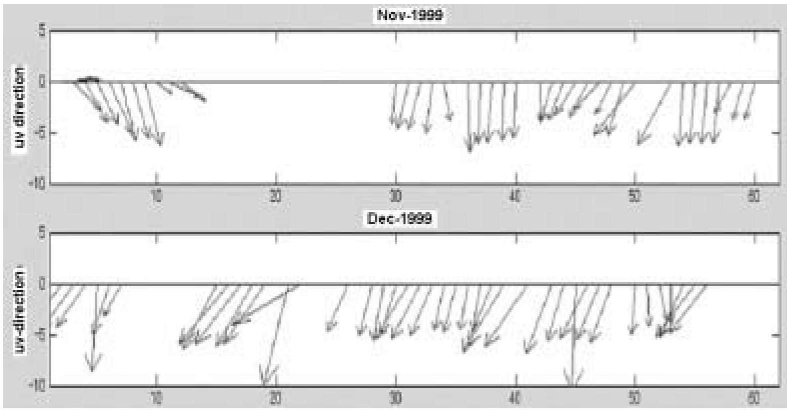

Figure 2a. Wind vectors over the Gulf of Kutch estimated from Quikscat data from Nov. to Dec 1999. Data are collected twice a day, and the number of data is taken on the abscissa.

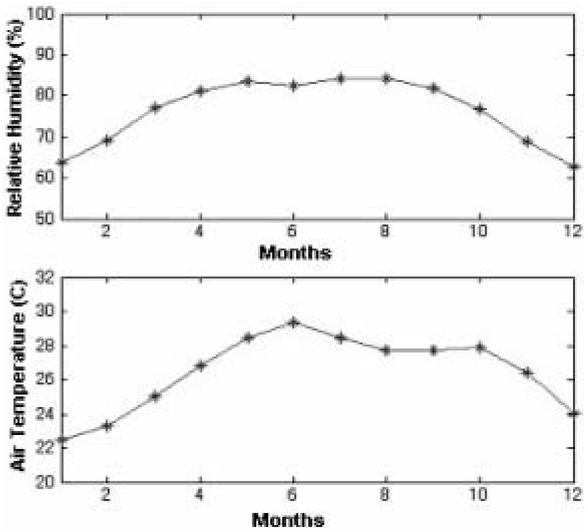

Figure 2b. Relative humidity (top) and air temperature (bottom) variation over the Gulf of Kutch obtained from Da SILVA *et a*l. (1994).

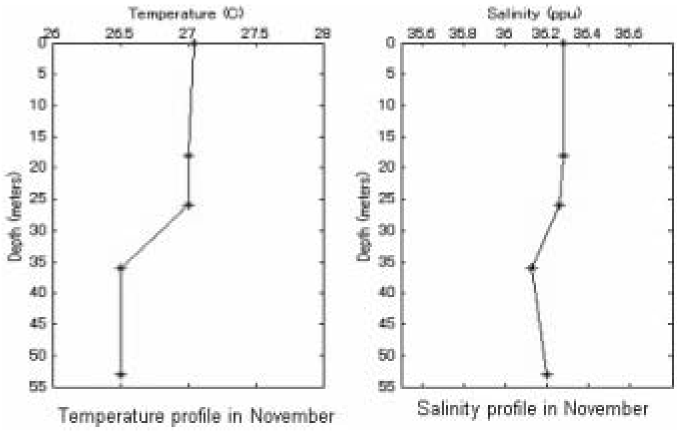

Figure 2c. Cloud fractions over the Gulf of Kutch in one year from Da Silver *et al.* (1994).

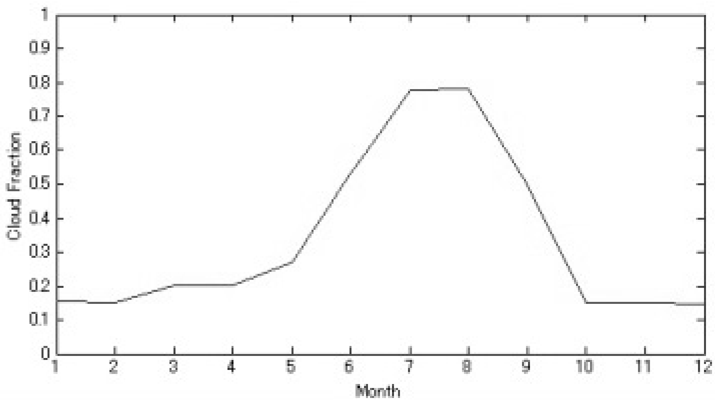

Figure 2d. Temperature and salinity profile measured at the open boundary of Gulf of Kutch.

Table 4. Mean wind velocity over the Gulf of Kutch from Quikscat data

	U m/s	V m/s	Speed
Nov 1999	−0.02	−4.14	4.1
De. 1999	−1.93	−5.45	5.8
Jan .2000	−0.10	−4.20	4.2
Feb. 2000	0.79	−3.94	4.0

length, cloud fraction, air temperature and relative humidity. In this study, wind data retrieved from Quickscat satellite are used because no in situ measurements were available. A Quickscat sensor was launched in 1999 as the successor of Japanese satellite ADEOS/NSCAT to monitor oceanic wind field globally. Map of ocean surface winds over global oceans twice a day derived from the observations by the SeaWinds scatterometer on Quickscat was interpolated and provided in wind grid data by JPL (TANG and LIU, 1996). Figure 2a shows the mean wind vector over the Gulf of Kutch from Nov. 1999 to Dec. 1999. In winter, wind velocity over the Gulf is less than 10 m/s and wind direction are generally from north. Table 4 lists the mean wind speed in the Gulf in winter season, and the mean value used in the model is 4.1 m/s.

Air temperature, relative humidity and cloud fraction are obtained from Da SILVA *et al.* (1994) climatic data sets from 1984–1991. Figure 2b shows the air temperature and the relative humidity above sea surface. We can see that the temperature changes from 22–29℃ with relative humidity variations between 60%

and 80%. Figure 2c shows the cloud fraction in this area and less than 20% cloud coverage from Oct. to May next year.

Figure 2d shows the profile of temperature and salinity measured at the open boundary in November 1997 near Okha. After checking the wind data and NOAA/AVHRR data and available in-situ data, the model calculation is conducted for Nov. 1999. The meteorological data chosen here are shown in Table 1. Surface solar irradiance in the Gulf of Kutch is calculated using the software written by PLATT *et al.* (2000).

4. Model results and discussions

The numerical experiment was conducted for the period starting from Nov. 1, 1999 for one month. As limited observations were carried out, sea surface temperature obtained from NOAA/AVHRR and results of earlier researches (SINHA *et al.* 2000, UNNIKRISHNAN *et al.* 1999) were used to validate the model results.

4.1 Surface current velocity distribution

Figure 3a and 3b (See P. 102) show the model results of ocean surface current velocities overlaid on the sea surface variation. Figure 3a is surface current distribution before high tide at the mouth of the Gulf. Surface variation changes from 0 cm at the bay head to 343 cm at the bay mouth and current travels from the mouth to the head of Gulf with maximum speed of 272 cm/s. Three hours later, the sea surface variation in the Gulf is from 250 cm at the bay mouth to 540 cm at the bay head with maximum current speed of 99 cm/s (Fig 3b). At this time, the tide in the mouth region has changed from 350 cm to 250 cm and that in the head region changes from 0 cm to 540 cm in 3 hours, and tidal current direction is reversed as compared with Figure 3a in the mouth region of the Gulf. As far as the tide magnitude is concerned, the model simulation shows that the maximum current velocity attains up to 270 cm/s. These results are almost the same with the other numerical results (SINHA *et al.* (2000), PRANDTL (1984)), which were estimated from 2D numerical model (Figure 4) (See P. 102) and only tidal influence included. However, the residual current field shows much more detailed structure in our 3D numerical models, especially we can find the difference of the residual currents in the vertical direction.

4.2 Residual current distribution

Residual current distribution in the Gulf of Kutch is shown in Figure 5a (See P. 102) gives the similar patterns as obtained by earlier studies (PRANDTL, 1984, SINHA *et al.*, 2000). Residual current travels from the mouth at the open boundary area with large magnitude around 15 cm/s, two largest residual current regions are found in the east and west of the Island Bural Chanka with a magnitude of more than 25 cm/s. However, on average, the residual currents have average magnitudes less than 5 cm/s as shown in Figure 5a.

A clear anti-cyclonic eddy of residual current is located near the mouth of the Gulf, which was also reported, by PRANDTL (1984), UNNIKRISHNAN *et al.* (2000) and SINHA *et al.* (2000). Several convergence and divergence regions are visible in the middle part of the Gulf. The main features of the residual current field do not show much difference amongst subsurface layers and bottom layer of the Gulf of Kutch. However, the current speed decreases from the surface to bottom layer. When compared with different water depth distribution, we found that the areas with larger value of residual current are located over the area with rapid depth change. Hence, it is concluded that topography is the most important factor in the Gulf of Kutch in determining the distribution of residual current velocity. UNNIKRISHNAN *et al.* (1999) also used model simulation to validate the effect that the topography on the eddy generation and showed that the eddy disappears if no depth variation is assumed in the model. Figure 5b and Figure 5c show the residual current distribution in the middle and bottom layer. Various features like eddy, places of convergence and divergence etc, which are visible in the surface layer, are seen diminishing towards deeper layers of the Gulf of Kutch. Hence, using 3D model study, it is easy to decipher the depth to which tides are influencing the water section.

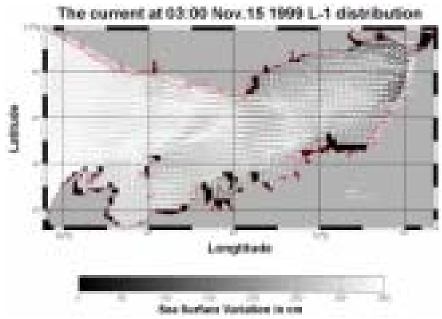

Figure 3a. Surface current velocity distribution from 3-D numerical model (before high tide at Okha around open boundary)

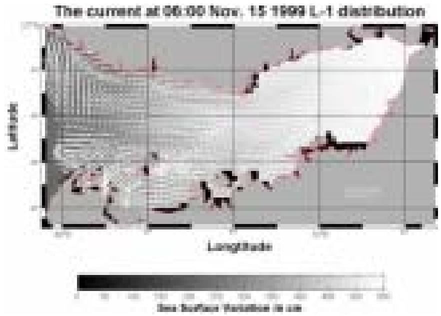

Figure 3b. Surface current velocity distribution from 3-D numerical model (after high tide at Okha)

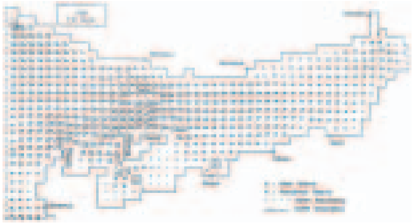

Figure 4. Tide stream current one and half hour before high at Okha (excerpted from Sinha *et al.* (2000)) .

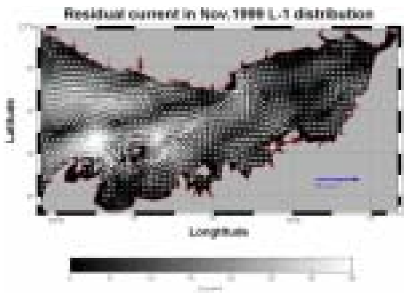

Figure 5a. Residual current velocity distribution of the Gulf of Kutch the first layer.

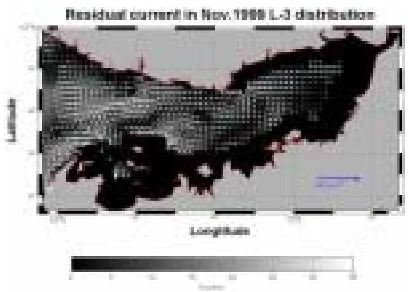

Figure 5b. Residual current velocity distribution of the Gulf of Kutch the Middle layer.

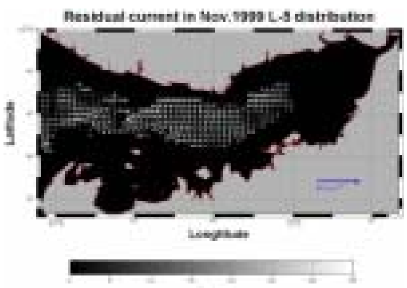

Figure 5c. Residual current velocity distribution of the Gulf of Kutch the bottom layer.

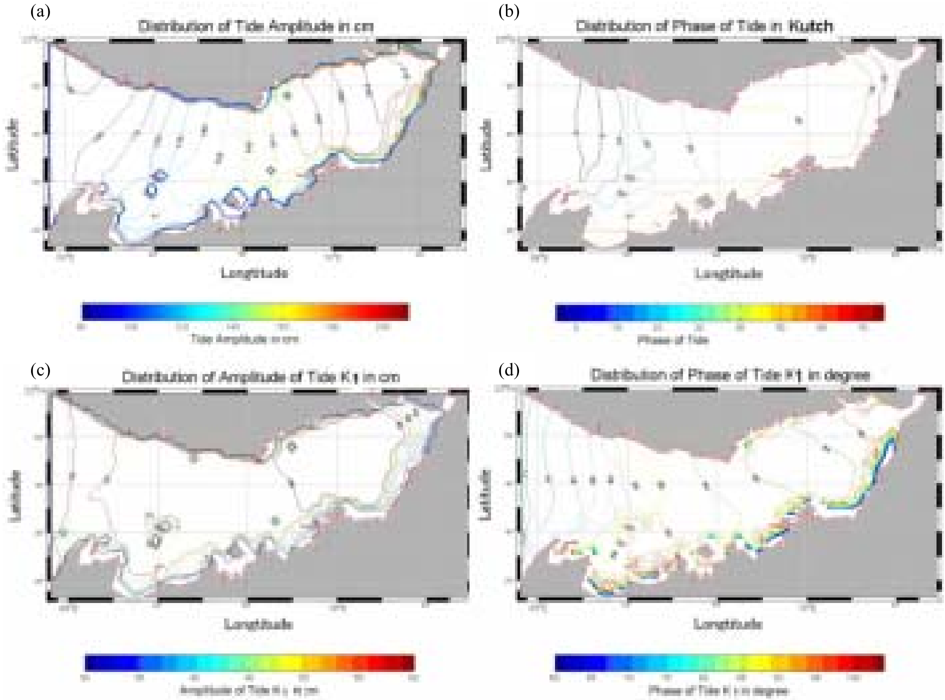

Figure 6. (a) Tide amplitude of M_2 in Gulf of Kutch, (b) Tide phase of M_2 in Gulf of Kutch, (c) Tide amplitude of K_1 in Gulf of Kutch, (d) Tide phase of K_1 in Gulf of Kutch

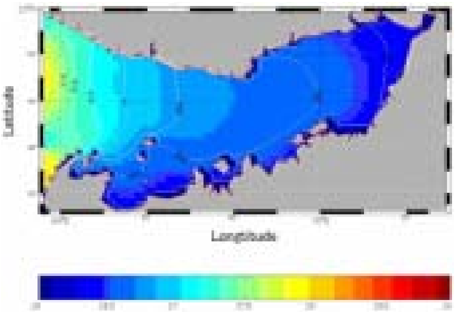

Figure 7a. Sea surface temperature in the first layer of the Gulf of Kutch

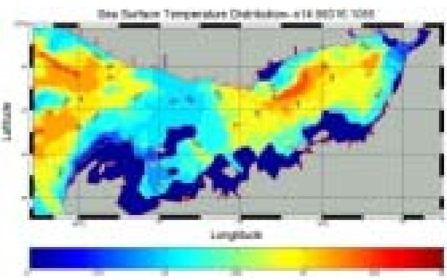

Figure 7b. Sea surface temperature measured by NOAA/AVHRR

4.3 Tidal features and tidal mixing effects

The main characteristic of Gulf of Kutch is its high tidal variation. SHETYE (1999) proposed that amplification of tide is due to a combination of quarter-wavelength resonance and geometric effect. We analyzed the model results and obtained the amplitude and phase distributions of tide M_2 and K_1 components for comparison. Figure 6a, b (See P. 103) shows that the amplification ratio for M_2 tide is about 2.3 times and the phase difference is about 90 degree. According to quarter-wavelength resonance condition, the tide period is equal to the resonance period $T_r = 4L/(gH)^{1/2}$, (L is wave length and H is wave height). The resonance period in the Gulf of Kutch is 16 hrs. After considering the bottom friction and other factors, SHETYE (1999) proposed that the resonance period is around 11.5 hrs, which is almost coincides with M_2 period and hence tidal amplification takes place. We also analyzed the second largest tide component, K_1, in Gulf of Kutch and the results (Figure 6c and Figure 6d) (See P. 103) shows that the tidal amplitude variation changes from 55 cm to 60 cm in the Gulf and phase difference is just 24 degrees. It concludes that no resonance effect was observed with K_1 tidal component. UNNIKRISHNAN *et al.* (1999) also noted this amplification effect and proposed the natural period as around 10 hr using moment balance along lateral section, which is also similar to our model simulations.

4.4 Sea surface temperature and salinity distribution

Sea surface temperature derived from NOAA/AVHRR was used to validate the model results, It is found that sea surface temperature decreases from the mouth toward the head of the Gulf after wind stress influence is considered in the model simulation. The similar trend was also found in NOAA/AVHRR data. However, the detailed structure of sea surface temperature differs as satellites measures the skin temperature of water body whereas the model considers entire first layer. The sea surface temperature obtained from NOAA/AVHRR, shown in Figure 7b, decreases from the mouth to the head of the Gulf, and our model results (Figure 7a) (See p. 103) also show the similar trend and pattern. Salinity distribution in the Gulf was also investigated using 3D numerical model. As we have no the in-situ data for the same season, we set the initial condition of salinity profile to be the same as the open boundary. The model results show salinity distribution in the Gulf varies from 36.09 to 36.13 psu, and no much difference is found after considering wind stress.

5. Conclusions

From COSMOS model results, it is concluded that the current system (tidal and residual tidal) is mainly controlled by tidal variation. In this study, wind stress slightly changes surface current pattern without disturbing major structure of current, as wind speed is generally very low in November. Current field in the subsurface are similar to surface current velocity distribution but are of lesser magnitude. Residual current velocity distribution shows a clear anti-cyclonic eddy, several divergence and convergence areas in the center of Gulf, which is not reported in earlier studies. Further in-situ investigations are needed to confirm their existence. Two areas with large magnitude of current velocity are found over the area with higher depth variation. It shows the importance of topography in controlling current fields.

Sea surface temperature decreases from the mouth toward the head of the Gulf after wind stress influence is considered in the model simulation. The similar trend was also found in NOAA/AVHRR data. However the detail structure of sea surface temperature differs as satellites measures the skin temperature of water body whereas the model considers entire first layer. Finally, the COSMOS model has achieved reasonable success in predicting hydrodynamic parameters in high tide dominated GoK. However use of higher spatial resolution and extensive incorporation of the spatially and temporally field data into the modeling process are required to be made to attain reality in the future.

Acknowledgements

Satellite wind data is obtained from the NASA/NOAA sponsored data system Seaflux, at JPL through the courtesy of W. Timothy Liu and Wenqing Tang, and climatic meteorological data is obtained from Da SILVA *et al.* (1994). Second author gratefully acknowledges Japan Society of Promotion of Science (JSPS), Japan for awarding RONPAKU Fellowship under which this work has been carried out.

References

CENTRAL ELECTRICITY AUTHORITY (1985): Investigations and studies for tidal power development in the Gulf of Kutch, Interim Rep. Ministry of Irrigation and Power, Government of India, New Delhi, pp. 87.

Da SILVA, A., A. C. YOUNG and S. LEVITUS (1994): Atlas of surface marine data 1994, Volume 1, Algorithms and procedures, Technical report 6, US Department of Commerce, NOAA, NESDIS 6, Washington D.C.

HORIGUCHI, F., K. NAKATA, P. LEE, W. CHOI, C. KIM, and T. TERASAWA, (1998a): Mathematical Eco-hydrodynamical model application in Chinhae Bay, J. Adv. Mar. Sci. Tech. Soci., **4 (1)**, 81–94.

HORIGUCHI, F., K. NAKATA, H. NISHIDA (1998b): The development of a size-based mathematical eco-hydrodynamical model and application to Tokyo Bay, J. Adv. Mar. Sci. Tech. Soc. **4 (1)**, 95–122.

NAKANO, S. (1936): Tide. published by Kokin Syoin (in Japanese), pp 528.

NAKATA, K., F. HORIGUCHI, and Y. SETOGUCHI (1983): Oinami Bay, 3-dimensional tidal simulation, Pollut. And Resc. **12 (3)** , 17–36.

PLATT T., S. SATHYENDRANATH, and G. WHITE, (2000) : Ocean Primary Production Software Package for Calculation of Oceanic Primary Production, Biological Oceanography, Ocean Sciences Division, Bedford Institute of Oceanography, Dartmouth, Nova Scotia, Canada.

PRANDTL, D., (1984) : Simple theory for designing tidal power scheme, Adv. Water Resources, **7**, 21 27.

SALOMON J. C. (1976): "Modele mathematique da la propagation da la maree en stuaire et des transports sableux associes. Application aux estuaries Da la Loire et Da la Seine" (in French), Ph.D thesis, Univ. De Nretagne Occidentale, Brest, France, pp. 257.

SHETYE, S. R. (1999), Tides in the Gulf of Kutch, India, Continental Shelf Research, **19**, 1771–1782.

SINHA, P. C., S. K. DUBE, A. K. MITRA and T. S. MURTY (2000): A tidal flow model for the Gulf of Kachchh, India, Marine Geodesy, **23**, 117–132.

TANG, W. and W. T. LIU (1996): Objective interpolation of scatterometer winds, JPL publication 19–96.

UNNIKRISHNAN, A. S., A. D. GOUVEIA, and P. VETHAMONY (1999): Tidal regime in Gulf of Kutch, west coast of India by 2D model, Journal of Waterway, Port, Coastal and Ocean Engineering, **125**(**6**) 276–284.

Received August, 26, 2002
Accepted August, 11, 2003